European Journal of Immunology

Tumor immunology

Basic

Short Communication

Gut microbiota alterations affect glioma growth and innate immune cells involved in tumor immunosurveillance in mice

Giuseppina D'Alessandro[*1,2], *Fabrizio Antonangeli*[*3], *Francesco Marrocco*[1,4], *Alessandra Porzia*[3], *Clotilde Lauro*[1], *Angela Santoni*[2,3] *and Cristina Limatola*[2,5]

[1] Department of Physiology and Pharmacology, Sapienza University, Rome, Italy
[2] IRCCS Neuromed, Pozzilli, IS, Italy
[3] Department of Molecular Medicine, Laboratory Affiliated to Istituto Pasteur Italia, Sapienza University, Rome, Italy
[4] Center for Life Nanoscience–IIT@Sapienza, Rome, Italy
[5] Department of Physiology and Pharmacology, Laboratory Affiliated to Istituto Pasteur Italia, Sapienza University, Rome, Italy

Glioma is a CNS tumor with few therapeutic options. Recently, host microbiota has been involved in the immune modulation of different tumors, but no data are available on the possible effects of the gut–immune axis on brain tumors. Here, we investigated the effect of gut microbiota alteration in a syngeneic (GL261) mouse model of glioma, treating mice with two antibiotics (ABX) and evaluating the effects on tumor growth, microbe composition, natural killer (NK) cells and microglia phenotype. We report that ABX treatment (i) altered the intestinal microbiota at family level, (ii) reduced cytotoxic NK cell subsets, and (iii) altered the expression of inflammatory and homeostatic proteins in microglia. All these findings could contribute to the increased growth of intracranial glioma that was observed after ABX treatment. These results demonstrate that chronic ABX administration alters microbiota composition and contributes to modulate brain immune state paving the way to glioma growth.

Keywords: Antibiotics · Glioma · Gut microbiota · Innate immunity · NK cells

Additional supporting information may be found online in the Supporting Information section at the end of the article.

Introduction

Glioma is the most frequent and lethal cancer in the adult CNS [1]. One key element of its recurrence is the immunosuppressive tumor microenvironment, which counteracts the host defense activities [2]. Glioma secretes molecules responsible for the recruitment of innate immune cells such as microglia and monocytes, which account to about 30% of the whole tumor mass and whose presence negatively correlates with patient's survival [3]. The panel of infiltrating immune cells also comprises T lymphocytes and natural killer (NK) cells [4, 5]. NK cells have direct cytotoxic activity against cancer cells [6], and their depletion hampers the

Correspondence: Cristina Limatola
e-mail: cristina.limatola@uniroma1.it

*Both authors contributed equally to this work.

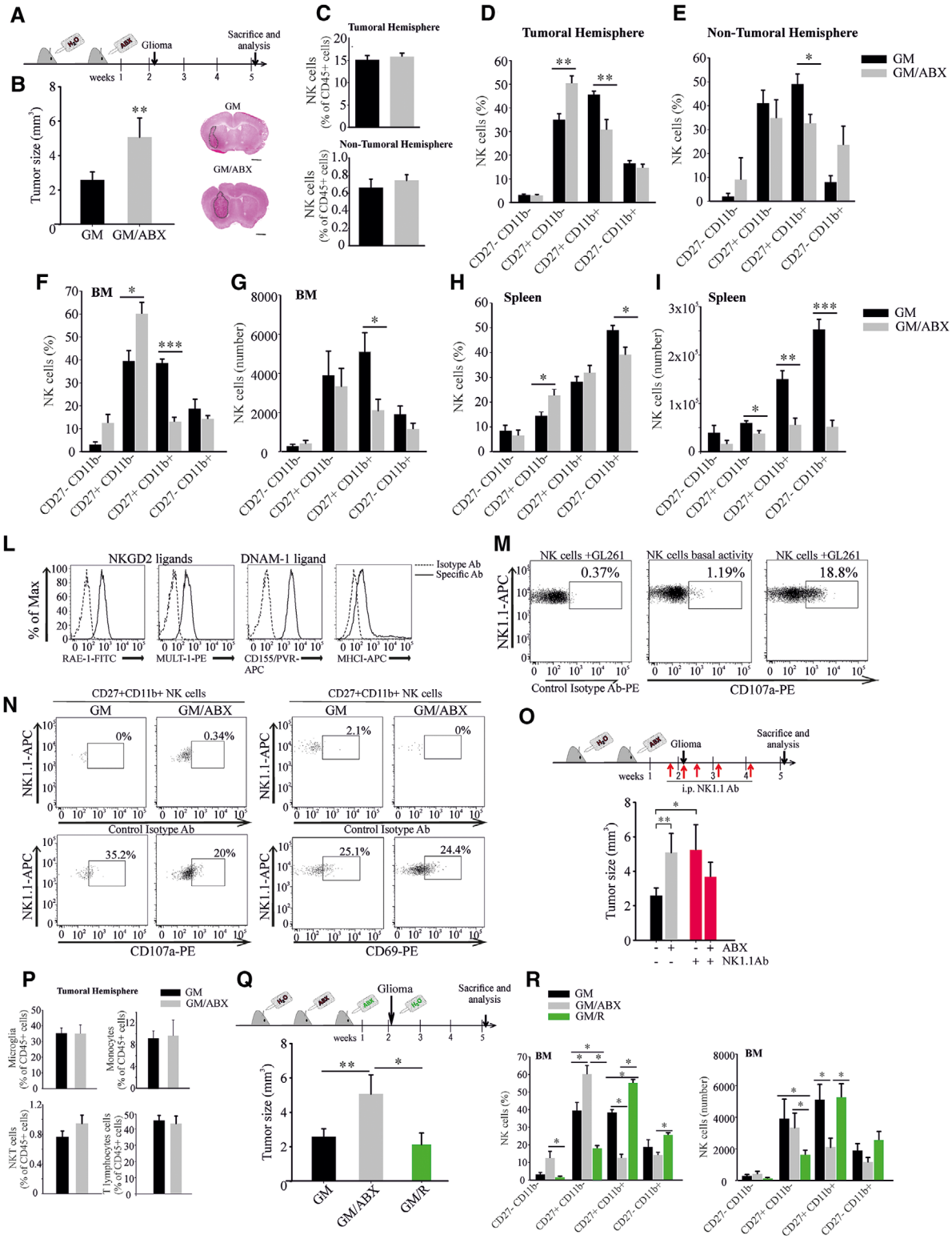

Figure 1. Tumor size and NK cell alterations in ABX-treated tumor-bearing mice. (A) Study design. (B) Tumor size in GM and GM/ABX mice, $n = 9$, pooled from three experiments, two to five animals per group. Right: Representative images of brain coronal slices, scale bar = 1 mm. (C–E) Flow cytometric analysis of NK cells in the brain and NK cell subset analysis of GM and GM/ABX mice. NK cells were gated as $CD45^+/CD3^-/NK1.1^+$ lymphocytes and divided according to CD27 and CD11b expression (C, top: GM $n = 10$, GM/ABX $n = 10$, pooled from five experiments, one to three animals per group; bottom: GM $n = 7$, GM/ABX $n = 4$ pooled from four experiments, one to three animals per group; (D) GM $n = 7$, GM/ABX $n = 7$ pooled from four experiments, one to three animals per group; (E) GM $n = 5$, GM/ABX $n = 3$ pooled from four experiments, one to two animals per group). (F, G) Percentage (GM $n = 5$, GM/ABX $n = 6$ pooled from three experiments, one to three animals per group) and absolute number

anti-cancer properties exerted by IL-15 and environmental stimuli in mouse models of glioma [7]. Heterogeneity of mouse NK cells encompasses distinct subsets endowed with different effector functions and characterized by the different expression of CD27 (CD70 receptor) and CD11b (integrin αM) [8]. The composition of gut microbiota (GM) is recognized as a key element that affects the host metabolism and the development and function of the immune system, playing important roles in systemic diseases and modulating brain functions [9, 10]. In the present study, we demonstrate that chronic ABX treatment alters the GM composition and promotes brain tumor growth, hampering cytotoxic NK cell subsets.

Results and discussion

Glioma growth increases in ABX-treated mice

Microbiota involvement in cancer patient's response to immune modulators has been recently demonstrated showing that chronic ABX consumption is associated with poor response in epithelial tumors [11]. An open unexplored question is the possibility to alter cerebral tumor microenvironment acting on gut microbe composition. To investigate if chronic ABX treatment could alter GM composition and impact glioma growth, we treated mice with two not orally absorbable ABX and after 2 weeks the syngeneic GL261 glioma cells (GM) were brain transplanted. Three weeks later, upon continuous ABX treatment, tumor size was evaluated (Fig. 1A). Data in Fig. 1B indicate that in ABX-treated mice (GM/ABX) tumor volume was significantly increased. Gut microbiota regulates the immune function [12], but the role of specific taxa or the mechanisms and metabolites involved need further investigation. Few studies investigated NK cell activity in germ-free conditions, showing altered NK cell cytotoxicity upon epigenetic remodeling [13] or reduced priming [14]. In our experiments, we observed that the frequency of NK cells ($CD45^+/CD3^-/NK1.1^+$) infiltrating the tumoral and the non-tumoral hemisphere was not modified by ABX treatment (Fig. 1C), while the cytotoxic $CD27^+/CD11b^+$ NK cell subset was reduced and the immature $CD27^+/CD11b^-$ NK cell population was increased (Fig. 1D and E). The effect on NK cell subsets was not tumor specific, since a reduced abundance of $CD27^+/CD11b^+$ NK cells was also measured in the bone marrow (BM) and the spleen (Fig. 1F–I). Because the $CD27^+/CD11b^+$ NK cells are involved in tumor cell lysis and control of metastasis [15, 16], we speculate that their reduction could explain tumor size increase observed in GM/ABX mice. We verified that GL261 cells were susceptible to NK cell lysis in vitro, measuring NKGD2 ligands (RAE-1 and MULT-1), DNAM ligand (CD155/PVR), and MHC class I expression and performing a degranulation assay (as CD107a expression, Fig. 1L and M). Also the CT-2A murine glioma cells were subject to NK cells cytotoxicity (data not shown). In addition, the $CD27^+/CD11b^+$ NK cell subset was effective in the tumor microenvironment, since they expressed CD107a (GM: 33.1 ± 7.6%; GM/ABX:17.5 ± 3.3%*, $p < 0.05$, $n = 4$ pooled from two experiments, two animals per group, *t*-test) and the activation marker CD69 (GM: 26.7 ± 2.4%; GM/ABX: 30.1 ± 2.7%, $n = 4$ pooled from two experiments, two animals per group) (Fig. 1N). This result shows that ABX treatment affected both the amount of mature NK cells and their cytotoxic activity. The functional impairment and the altered immature/mature NK cell ratio have been involved in a murine model of MS [17]. To investigate a direct link between tumor growth and NK cell activity, we depleted NK cells from GM and GM/ABX mice (supporting gating strategy, D for NK cell depletion checking) and evaluated tumor size. As shown in Fig. 1O, NK cell depleted GM mice had bigger tumor compared to non-depleted mice, confirming the antitumoral activity of NK cells in glioma. In neuroinflammation, the cross-talk of NK cells with infiltrating monocytes is neuroprotective [18]. We did not observe differences in frequency of microglia ($CD45^{low}/CD11b^+/Ly6C^-/Ly6G^-$), monocytes/macrophages ($CD45^+/CD11b^+/Ly6C^+$), or infiltrating lymphocytes such as T ($CD45^+/CD3^+$) and NKT ($CD45^+/CD3^+/NK1.1^+$) cells in the tumoral hemisphere upon ABX treatment (Fig. 1P). Recent papers described that an enriched environment promotes NK cell maturation and enhances their antitumor immunity via sympathetic nerve-dependent regulation of NKG2D and CCR5 [19, 20] and through IFN-γ-mediated communication with microglia [21]. To further demonstrate that changes in gut microbiota could affect tumor growth, ABX treatment was interrupted for some mice, allowing gut microbiota recovery (GM/R) (Fig. 1Q). This treatment reduced tumor size and reverted the effects on NK cell subset distribution compared to mice continuously treated with ABX (Fig. 1Q and R). These data suggest a role of microbiota in shaping NK cell population and thus the anti-tumoral activity in glioma.

(GM $n = 8$, GM/ABX = 12 pooled from five experiments, one to four animals per group) of NK cell subsets in the BM. (H, I) Percentage (GM $n = 7$, GM/ABX $n = 7$ pooled from four experiments, one to three animals per group) and absolute number (GM $n = 5$, GM/ABX $n = 6$ pooled from four experiments, one to two animals per group) of NK cell subsets in the spleen. (L) Flow-cytometric analysis of NK cell activating ligands and MHC class I expression in murine GL261 cells. (M) NK cell degranulation activity against GL261 cells. (N) Activation status of $CD27^+CD11b^+$ NK cells in the tumoral hemispheres of GM and GM/ABX mice (representative experiment). (O) Upper: Study design of in vivo NK cell depletion; lower: tumor size in NK cell–depleted GM and GM/ABX mice, $n = 5$ per group pooled from two experiments, two to three animals per group. (P) Upper left: Flow cytometric quantification of microglia defined as $CD45^{low}/CD11b^+/Ly6C^-/Ly6G^-$ population ($n = 7$ pooled from four experiments, one to three animals per group); upper right: brain-associated monocytes/macrophages defined as $CD45^+/CD11b^+/Ly6C^+$ (GM $n = 7$, GM/ABX $n = 5$ pooled from four experiments, one to two animals per group); lower left: NKT lymphocytes ($CD45^+/CD3^+/NK1.1^+$; GM $n = 7$, GM/ABX $n = 5$ pooled from four experiments, one to two animals per group); lower right: T lymphocytes ($CD45^+/CD3^+/NK1.1^-$; GM $n = 7$, GM/ABX $n = 5$ pooled from four experiments, one to two animals per group). (Q) Upper: Study design of gut microbiota recovery; lower: tumor size in GM, GM/ABX ($n = 9$ pooled from three experiments, two to five animals per group) and GM/R (microbiota restored mice, n = 5 pooled from two experiments, two to three animals per group). *$p < 0.05$, ** $p < 0.01$, *** $p < 0.001$ by multiple Student's *t*-test or ANOVA.

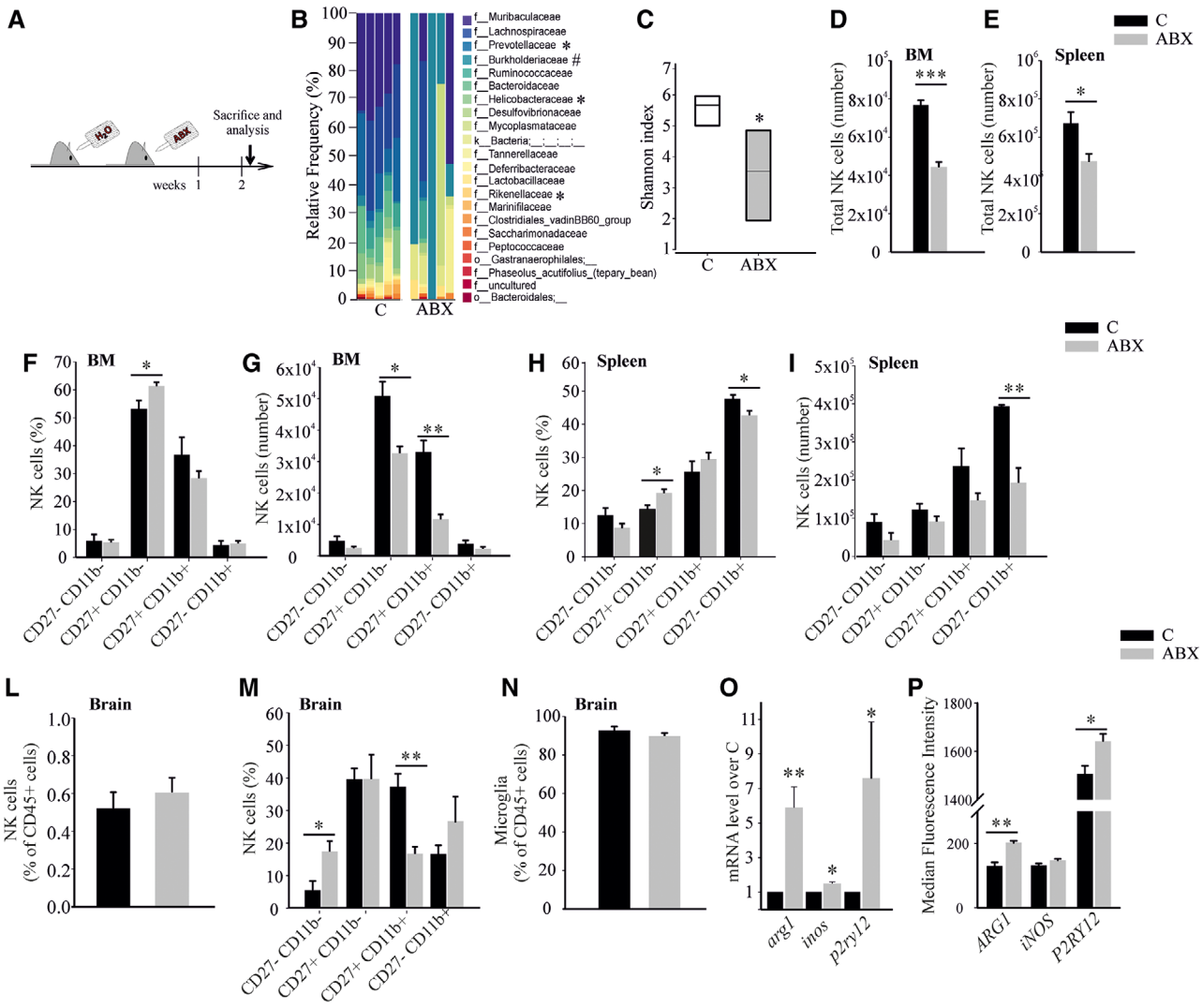

Figure 2. ABX administration alters gut microbiota composition and hampers NK cells. (A) Study design. (B) Family-level phylogenetic classification of cecal 16S rDNA gene frequencies from control or 2-week ABX-treated mice. Each bar represents one mouse, $n = 5$ pooled from two experiments, two to three animals per group, *decreased or #increased versus control by ANCOM analysis. **(C)** Quantitative analysis of α-diversity of the gut microbiota in ABX-treated mice compared to controls, $n = 5$ pooled from two experiments, two to three animals per group, $^{*}p < 0.05$ by Kruskal–Wallis test. **(D, E)** Total number of NK cells in the BM (C = 5, ABX = 5 pooled from four experiments, one to two animals per group) and spleen (C = 7, ABX = 10 pooled from three experiments, one to four animals per group). **(F–I)** NK cell subset analysis in the BM and spleen of control and ABX mice (**F**, C = 4, ABX = 7 pooled from two experiments, two to four animals per group; **(G)** C = 5, ABX = 4 pooled from two experiments, two to three animals per group; **(H)** C = 4, ABX $n = 7$ pooled from two experiments, two to four animals per group; **(I)** C = 4, ABX = 4 pooled from two experiments, two animals per group). **(L, M)** NK cell percentage (C = 8 and ABX = 10 pooled from four experiments, one to three animals per group) and NK cell subset distribution (C = 4 and ABX = 4 animals pooled from three experiments, one to two animals per group) in the brain of treated mice. **(N)** Microglia quantification by flow cytometry (C = 8, ABX = 10 pooled from five experiments, one to three animals per group). **(O)** mRNA level as fold increase in ABX mice over control mice, $n = 6$–7 pooled from three experiments, two to three animals per group. **(P)** Protein expression level (MFI) as evaluated by flow cytometric analysis, n = 5 pooled from two experiments, two to three animals per group. $^{*}p < 0.05$, $^{**}p < 0.01$, $^{***}p < 0.001$ by multiple Student's *t*-test.

ABX administration alters gut microbiota and innate immune cells

We investigated the effects of ABX treatment on gut microbiota and innate immune cells at the moment of glioma transplantation (Fig. 2A). Phylogenetic analysis of cecal microbiota of ABX-treated mice showed increase of Burkholderiales families (Alcaligenaceae and Burkholderiaceae) and reduction of the Prevotellaceae, Rikenellacaea, and Helicobacteraceae families (Fig. 2B). ABX mice also showed an overall reduction in species diversity, as a lower α-diversity Shannon index (Fig. 2C). NK cells from the BM and the spleen of control and ABX-treated mice were analyzed: Figure 2D–I shows that 2-week ABX treatment modified NK cells number and the subset distribution. This effect was specific for NK cells since the number of splenic B lymphocytes ($CD45^{+}/CD19^{+}$ cells) and resident DCs

($CD45^+/CD11c^+$ cells) was not affected (not shown) [22]. The frequency of NK cells in the brain was not modified by ABX treatment (Fig. 2L). Nevertheless, and consistent with the data on BM and spleen, ABX treatment reduced the frequency of $CD27^+/CD11b^+$ cell subset (Fig. 2M). A microbe–microglial communication has been recently described [9], with key role played by short chain fatty acids. ABX treatment did not change microglia frequency (Fig. 2N) but the $CD11b^+$ cells (mainly microglia) isolated from the brain of ABX-treated mice modulated the expression of genes involved in the immune functions [23] and in patrolling activity [24]. ABX treatment increased *arg1*, *p2ry12*, and *inos* mRNA expression and ARG1 and P2RY12 proteins in microglia (Fig. 2O and P), indicating a different activation state and, likely, inflammatory activity.

Concluding remarks

Here we demonstrated that ABX-treatment of glioma-bearing mice promoted tumor growth and changed the NK cell subsets and effector functions in the brain, BM, and spleen. We also demonstrated that ABX treatment modified gut microbiota, induced early impairment of NK cells, and induced changes in microglia phenotype, suggesting that an altered gut–immune–brain communication may contribute to induce a tumor-tolerant CNS microenvironment, which favors tumor development. Further experiments will be necessary to investigate how microbiota alterations modulate the activity of innate immunity. Here, we speculate that the absence of microbial signals from Prevotellaceae, Rikenellacaea, and Helicobacteraceae or the increased signals from Burkholderiales are responsible for the observed effects. It is possible that an altered microbiota can modulate the systemic inflammatory state that is mediated by microbiota-regulated signals such as pattern recognition receptors (PPRs) or IFN-I. Altogether, these data support the presence of a functional gut–immune–brain axis whose modulation might represent a tool to counteract brain tumor immunosuppression.

Materials and methods

Animal husbandry

C57BL/6N mice (males, 6 weeks) were randomly assigned to experimental groups. The microbiological status of the animals and facility (in Sapienza University) is continuously monitored. All mice were housed (two to four animals per cage) under a 12-h light cycle in standard cages, in autoclaved bedding and drinking water, and with sterilized standard chow ad libitum.

GL261 transplantation and ABX treatment

The study was conducted in accordance with the ARRIVE guidelines [25]. All the experiments and procedures were approved by the Italian Ministry of Health (authorization No. 231/2015PR) in accordance with the EC Council Directive 2010/63/EU and the Italian D.Leg.26/2014. All the efforts were done to minimize animal suffering, and to reduce the number of animals, calculating the necessary sample size before starting the experiments. Glioma syngeneic mouse model and NK cell depletion were obtained as previously described [21]. Mice were treated with not-absorbable ABX ([0.5g/L] vancomycin and [0.5g/L] gentamicin) and sucralose (0.5%) to improve palatability or with sucralose alone (control solution) in autoclaved water. ABX and control solutions were changed every 2 days. After 5-week ABX treatment, mice showed a slight but significant increase in body weight compared to controls (growth rates: C 111.0 $\pm$ 1.2%; ABX 115 $\pm$ 0.7%, $n = 5$ pooled from two experiments, two to three animals per group $p < 0.001$ by *t*-test).

Phylogenetic analysis

Bacterial DNAs from ceca were extracted with the Qiagen mini-stool-kit (Hilden, Germany) according to manufacturer's instructions. Ribosomal 16S DNA was amplified as in Ref. [26] and tested in 1.5% agarose gel. The taxonomies of Silvav.132 have been associated with OTU sequences. The alpha-diversity analyses were performed using the Shannon index; Kruskal–Wallis test was used to compare treatments. Differentially abundant microbial families were identified by ANCOM statistics.

Cell isolation and flow cytometric analyses

The study was conducted in accordance with the reported flow cytometry guidelines [27]. Single-cell suspensions were obtained from total brain, non-tumoral or tumoral hemispheres as indicated. Mice were intracardially perfused with PBS and brains were rapidly removed, hemispheres separated, and placed into ice-cold HBSS. The hemispheres were disrupted in a glass-teflon homogenizer and passed through a 100 μm nylon cell strainer (Becton-Dickinson). Suspension was centrifuged (800 *g*, 10 min, RT), the pellet was resuspended in 8 mL of 30% Percoll (Sigma) and overlaid on the top of HBSS. The suspension was centrifuged (14 000 *g*, 15 min, RT), the pellet was washed with 10% FBS in HBSS and cells used for flow cytometry or labeled with CD11b+ Microbeads and passed through MACS Columns (Miltenyi Biotec). Cells from the BM (one femur and tibia) and spleen were obtained by flushing with syringe and smashing on a 70 μm cell strainer, respectively. For flow cytometry, conjugated mAbs for the following antigens (clone name) were used: CD45.2-APC-eFluor780 (104), CD3e-PerCP-Cyanine5.5 (145-2C11), NK1.1-PE (PK136), NK1.1-APC (PK136), CD27-APC (LG.7F9), CD27-FITC (LG.7F9), CD11b-FITC (M1/70), CD11c-PE (N418), CD107a-PE (1D4B), ARG1 APC (A1exF5), Inos-PE (CXNFT) from eBioscience; CD19-FITC (6D5), CD11b-PE-Cy7 (M1/70), Ly6C-APC (HK1.4), Ly6G-PE (1A8), CD69-PE (H1.2F3), GR1-FITC (RB6-8C5), MHC class I/H-$2K^b$/H-2Db-APC (28-8-6), P2RY12-APC (S16007D) from BioLegend; RAE-1FITC (186107), MULT-1-PE (237104), CD155/PVR-APC

(690912) from R&D System. Cells were washed and suspended in staining buffer (PBS, 0.5% BSA, 2mM EDTA, 0.025% NaN_3). Anti-CD16/32 (clone 24G2) was added (10 min) to prevent non-specific and Fc-mediated binding. Cells were stained with the indicated antibodies for 20 min at 4°C. iNOS and ARG1 intracellular staining was carried out using the BD Cytofix/Cytoperm™ kit. NK cell degranulation assay was performed as previously reported with GL261 cells as target [28]. Samples were analyzed by FACS-CantoII (BDBiosciences) and data elaborated using FlowJo9.3.2 (TreeStar). Absolute number of cells was calculated as percentage multiplied by organ count. Gating strategies are shown in Supporting Information.

Tumor volume evaluation

Serial 20 μm coronal brain slices (one every 100 μm of entire tumor length) were collected and stained with standard H&E protocol. Tumor volume was calculated according to the formula (volume $= t \times \Sigma A$), where A is the tumor area/slice and t is the thickness by ImageTool3.0 software.

RNA preparation and qRT-PCR

Total RNA was isolated from $CD11b^+$ cells as previously described [21]. For quantification, the comparative threshold cycle (Ct) method was used. Ct values of each gene were normalized to Gapdh in the same RNA sample. Gene expression levels were evaluated as fold-change using the equation 2^{-ddCt}. The primers used were previously described [21].

Statistics

Data are expressed as mean ± SEM. Student's t-test or ANOVA was performed. The p value of <0.05 was considered statistically significant. Statistics were carried out by SigmaPlot11.0 (Systat Software GmbH, Germany) and Prism6.0 (GraphPad Software).

Acknowledgements: This work was supported AIRC2015/AIRC2019 to C.L. (IG-16699 and IG-23010) and Euronanomed III to A.S.

Conflict of interest: The authors declare no commercial or financial conflict of interest.

References

1 **Louis, D. N., Ohgaki, H., Wiestler, O. D., Cavenee, W. K., Burger, P. C., Jouvet, A., Scheithauer, B. W. et al.**, The 2007 WHO classification of tumours of the central nervous system. *Acta Neuropathol.* 2007. **114**: 97–109.

2 **Xie, Q., Mittal, S. and Berens, M. E.**, Targeting adaptive glioblastoma: an overview of proliferation and invasion. *Neuro-oncology* 2014. **16**: 1575–1584.

3 **Okada, M., Saio, M., Kito, Y., Ohe, N., Yano, H., Yoshimura, S., Iwama, T. et al.**, Tumor-associated macrophage/microglia infiltration in human gliomas is correlated with MCP-3, but not MCP-1. *Int. J. Oncol.* 2009. **34**: 1621–1627.

4 **Dunn, G. P., Dunn, I.F. and Curry, W. T.**, Focus on TILs: prognostic significance of tumor infiltrating lymphocytes in human glioma. *Cancer Immun.* 2007. **7**: 12.

5 **Kmiecik, J., Gras Navarro, A., Poli, A., Planaguma, J.P., Zimmer, J. and Chekenya, M.**, Combining NK cells and mAb9.2.27 to combat NG2-dependent and anti-inflammatory signals in glioblastoma. *Oncoimmunology* 2014. **3**: e27185.

6 **Lion, E., Smits, E. L., Berneman, Z. N. and Van Tendeloo, V. F.**, NK cells: key to success of DC-based cancer vaccines? *Oncologist* 2012. **17**: 1256–1270.

7 **Garofalo, S., D'Alessandro, G., Chece, G., Brau, F., Maggi, L., Rosa, A., Porzia, A. et al.**, Enriched environment reduces glioma growth through immune and non-immune mechanisms in mice. *Nat. Commun.* 2015. **6**: 6623.

8 **Chiossone, L., Chaix, J., Fuseri, N., Roth, C., Vivier, E. and Walzer, T.**, Maturation of mouse NK cells is a 4-stage developmental program. *Blood* 2009. **113**: 5488–5496.

9 **Erny, D., Hrabe de Angelis, A. L., Jaitin, D., Wieghofer, P., Staszewski, O., David, E., Keren-Shaul, H. et al.**, Host microbiota constantly control maturation and function of microglia in the CNS. *Nat. Neurosci.* 2015. **18**: 965–977.

10 **Frohlich, E. E., Farzi, A., Mayerhofer, R., Reichmann, F., Jacan, A., Wagner, B., Zinser, E. et al.**, Cognitive impairment by antibiotic-induced gut dysbiosis: analysis of gut microbiota-brain communication. *Brain Behav. Immun.* 2016. **56**: 140–155.

11 **Routy, B., Le Chatelier, E., Derosa, L., Duong, C. P. M., Alou, M. T., Daillere, R. et al.**, Gut microbiome influences efficacy of PD-1-based immunotherapy against epithelial tumors. *Science* 2018. **359**: 91–97.

12 **Clavel, T., Gomes-Neto, J. C., Lagkouvardos, I. and Ramer-Tait, A.E.**, Deciphering interactions between the gut microbiota and the immune system via microbial cultivation and minimal microbiomes. *Immunol. Rev.* 2017. **279**: 8–22.

13 **Poupeau, A., Garde, C., Sulek, K., Citirikkaya, K., Treebak, J. T., Arumugam, M., Simar, D. et al.**, Genes controlling the activation of natural killer lymphocytes are epigenetically remodeled in intestinal cells from germ-free mice. *FASEB J.* 2019. **33**: 2719–2731.

14 **Ganal, S. C., Sanos, S. L., Kallfass, C., Oberle, K., Johner, C., Kirschning, C., Lienenklaus, S. et al.**, Priming of natural killer cells by nonmucosal mononuclear phagocytes requires instructive signals from commensal microbiota. *Immunity* 2012. **37**: 171–186.

15 **Ballas, Z. K., Buchta, C. M., Rosean, T. R., Heusel, J. W. and Shey, M. R.**, Role of NK cell subsets in organ-specific murine melanoma metastasis. *PLoS One* 2013. **8**: e65599.

16 **Paul, S., Kulkarni, N., Shilpi and Lal, G.**, Intratumoral natural killer cells show reduced effector and cytolytic properties and control the differentiation of effector Th1 cells. *Oncoimmunology* 2016. **5**: e1235106.

17 **Hertwig, L., Hamann, I., Romero-Suarez, S., Millward, J. M., Pietrek, R., Chanvillard, C., Stuis, H. et al.**, CX3CR1-dependent recruitment of mature NK cells into the central nervous system contributes to control autoimmune neuroinflammation. *Eur. J. Immunol.* 2016. **46**: 1984–1996.

18 **Jiang, W., Li, D., Han, R., Zhang, C., Jin, W. N., Wood, K., Liu, Q. et al.**, Acetylcholine-producing NK cells attenuate CNS inflammation via

modulation of infiltrating monocytes/macrophages. *Proc. Natl. Acad. Sci. USA* 2017. **114**: E6202–E6211.

19 **Meng, Z., Liu, T., Song, Y., Wang, Q., Xu, D., Jiang, J. and Li, M.**, Exposure to an enriched environment promotes the terminal maturation and proliferation of natural killer cells in mice. *Brain Behav. Immun.* 2019. **77**: 150–160.

20 **Song, Y., Gan, Y., Wang, Q., Meng, Z., Li, G., Shen, Y., Wu, Y. et al.**, Enriching the housing environment for mice enhances their NK cell antitumor immunity via sympathetic nerve-dependent regulation of NKG2D and CCR5. *Cancer Res.* 2017. **77**: 1611–1622.

21 **Garofalo, S., Porzia, A., Mainiero, F., Di Angelantonio, S., Cortese, B., Basilico, B., Pagani, F. et al.**, Environmental stimuli shape microglial plasticity in glioma. *Elife* 2017. **6**. https://doi.org/10.7554/eLife.33415

22 **Hansson, J., Bosco, N., Favre, L., Raymond, F., Oliveira, M., Metairon, S., Mansourian, R. et al.**, Influence of gut microbiota on mouse B2 B cell ontogeny and function. *Mol. Immunol.* 2011. **48**: 1091–1101.

23 **Rath, M., Muller, I., Kropf, P., Closs, E.I. and Munder, M.**, Metabolism via arginase or nitric oxide synthase: two competing arginine pathways in macrophages. *Front. Immunol.* 2014. **5**: 532.

24 **Butovsky, O., Jedrychowski, M. P., Moore, C. S., Cialic, R., Lanser, A. J., Gabriely, G., Koeglsperger, T. et al.**, Identification of a unique TGF-beta-dependent molecular and functional signature in microglia. *Nat. Neurosci.* 2014. **17**: 131–143.

25 **Kilkenny, C., Browne, W. J., Cuthill, I. C., Emerson, M. and Altman, D. G.**, Improving bioscience research reporting: the ARRIVE guidelines for reporting animal research. *PLoS Biol.* 2010. **8**: e1000412.

26 **Takahashi, S., Tomita, J., Nishioka, K., Hisada, T. and Nishijima, M.**, Development of a prokaryotic universal primer for simultaneous analysis of bacteria and archaea using next-generation sequencing. *PLoS One* 2014. **9**: e105592.

27 **Cossarizza, A., Chang, H. D., Radbruch, A., Acs, A., Adam, A., Adam-Klages, S., Agace, W. et al.**, Guidelines for the use of flow cytometry and cell sorting in immunological studies (second edition). *Eur. J. Immunol.* 2019. **49**: 1457–1973.

28 **Antonangeli, F., Soriani, A., Ricci, B., Ponzetta, A., Benigni, G., Morrone, S., Bernardini, G. et al.**, Natural killer cell recognition of in vivo drug-induced senescent multiple myeloma cells. *OncoImmunology* 2016. **5**(10): e1218105.

Full correspondence: Cristina Limatola, Department of Physiology and Pharmacology, Laboratory Affiliated to Istituto Pasteur Italia, Sapienza University, Piazzale Aldo Moro 5, 00185 Rome, Italy
e-mail: cristina.limatola@uniroma1.it

The peer review history for this article is available at https://publons.com/publon/10.1002/eji.201948354

Received: 15/8/2019
Revised: 30/12/2019
Accepted: 5/2/2020
Accepted article online: 8/2/2020